

Photoinduced Superparamagnetism in Trimetallic Coordination Nanoparticles

Daniela Brinzei,[†] Laure Catala,^{*,†} Corine Mathonière,[‡] Wolfgang Wernsdorfer,[§] Alexandre Gloter,[¶] Odile Stephan,[¶] and Talal Mallah^{*,†}

Institut de Chimie Moléculaire et de Matériaux d'Orsay, CNRS, Université Paris Sud, 91405 Orsay Cedex, France, ICMCB, UPR CNRS 9048, Université Bordeaux 1, 87 avenue du Docteur Albert Schweitzer, F-33 608 Pessac Cedex, France, Institut Néel, CNRS, BP 166, 25 Avenue des Martyrs, 38042 Grenoble Cedex 9, France, and Laboratoire de Physique des Solides, UMR CNRS 8502, Université Paris Sud, 91405 Orsay Cedex, France

Received December 4, 2006; E-mail: laurecatala@icmo.u-psud.fr; mallah@icmo.u-psud.fr

The field of coordination nanoparticles (CNP) emerged only a few years ago due to the work of Mann on the stabilization of Prussian Blue analogue (PBA) nanocrystals.¹ PBAs offer many examples of bistability that can be tuned by field, light, temperature, or pressure.² One of the main objectives is to study the effect of size reduction on the cooperative properties of coordination networks. To date, efforts have mainly focused on ferromagnetic PBAs to achieve superparamagnetic CNP.^{3a,d–n} Different techniques, apart from reverse micelles, were used to efficiently control the growth of CNP.^{3b–n} Very recently, electrostatic stabilization of 6 nm superparamagnetic CrNi PBA nanoparticles was achieved in water.^{3k} Photomagnetic CoFe PBA nanoparticles were also reported.^{4a} However, light-induced superparamagnetic behavior was not examined on these nanoparticles. Cu₂Mo(CN)₈ photomagnetic nanorods were already stabilized.^{4b} However, no superparamagnetic properties were evidenced. In order to reveal such properties, we replaced half of the Cu^{II} ions with Ni^{II} that possesses a single ion magnetic anisotropy lacking in Cu^{II}. Indeed, anisotropy is a prerequisite to induce long relaxation times of magnetization and superparamagnetic behavior. In this communication, we report the first example of photoinduced superparamagnetism in 3 nm CuNiMo(CN)₈ trimetallic CNP.

Poly(vinyl pyrrolidone) (PVP), an organic polymer, was used to confine the growth of the coordination network and stabilize the nanoparticles.^{4b} An aqueous solution containing CuCl₂ (2 mM), NiCl₂ (2 mM), and PVP K30 was prepared in a ratio of [pyr]/[Cu²⁺] = 200 (where pyr stands for the monomer of PVP). The addition of an equivalent volume of a 2 mM K₄Mo(CN)₈ aqueous solution resulted in an immediate color change to violet. The mixture was left still for 1 h, and then the particles were recovered by precipitation in acetone. The precipitate that consists of the nanoparticles embedded in PVP was subsequently checked to determine if it was dispersible in water and ethanol. Elemental analysis performed on the precipitate that was dried and used for all of the studies gave the following composition: CuNiMo(CN)₈(pyr)₄₇·59H₂O (see Supporting Information).

The dynamic light scattering measurement performed on the redispersed precipitate revealed the presence of 8 nm nanoparticles that include PVP and solvation shells. The IR spectrum shows the asymmetric vibration of bridging cyanides at 2158 cm⁻¹, which lies between the Mo–CN–Cu (2163 cm⁻¹) and the Mo–CN–Ni (2154 cm⁻¹) bands present in the bulk compounds and evidences the presence of both metals. The UV–vis spectrum shows the presence of the intervalence band Mo(IV)Cu(II) → Mo(V)Cu(I) at 255 nm ($\epsilon = 402 \text{ L}\cdot\text{mol}^{-1}\cdot\text{cm}^{-1}$ per CuNiMo(CN)₈ entity, Figure

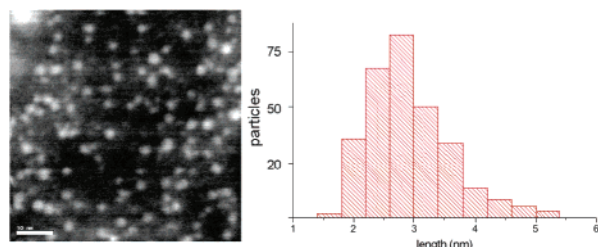


Figure 1. STEM image of CuNiMo(CN)₈ nanoparticles coated with PVP (scale bar = 10 nm) and size distribution.

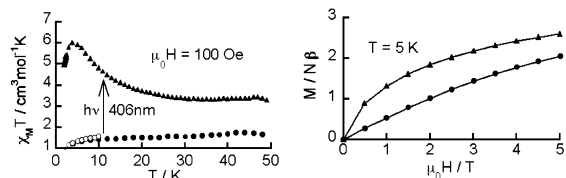


Figure 2. Thermal dependence of $\chi_M T$ before irradiation (●), after irradiation at $T = 10 \text{ K}$ (▲), and after thermal relaxation (○) at $T = 300 \text{ K}$ (left); $M = f(\mu_0 H)$ before (●) and after (▲) irradiation (right).

S1),^{4c} with a bathochromic shift of 18 nm compared to the Cu₂Mo(CN)₈ nanoparticles. The nanoparticles were imaged using dark field scanning transmission electronic microscopy (STEM) (Figure 1).

The statistics performed on 303 particles revealed a narrow size distribution centered on 2.9 nm ($\sigma = 0.7 \text{ nm}$), demonstrating that most of the nanocrystals correspond to giant clusters made of around 55 NiCuMo units. Electron energy loss spectroscopy (EELS) revealed the presence of both nickel and copper in the particles. The presence of nickel plays a drastic role on the growth process since nanorods ($10 \times 10 \times 70 \text{ nm}$) of Cu₂Mo(CN)₈ were obtained in the absence of nickel.^{4b} The nucleation step seems to be well separated from the growth step as a narrow size distribution of particles below 3 nm was obtained. Kinetic studies of nucleation and growth are in progress to evidence these assumptions.

The magnetic properties were studied on the nanoparticles before and after light irradiation (406–415 nm, power $\sim 7 \text{ mW}\cdot\text{cm}^{-2}$; see Supporting Information). Due to the presence of isolated paramagnetic Cu(II) and Ni(II), a paramagnetic behavior is observed before irradiation. Light irradiation induces an electron transfer from Mo(IV) to Cu(II) and generates ferromagnetically coupled Mo(V)/Ni(II) pairs confirmed by the increase of $\chi_M T$ upon cooling (Figure 2, left). The photoinduced ferromagnetic interaction is evidenced by the increased magnetization values at $T = 5 \text{ K}$ after irradiation (Figure 2, right). It reaches $2.5 \mu_B$ at $H = 5 \text{ T}$, close to the saturation value expected for the CuNiMo(CN)₈ unit formula ($3 \mu_B$). The photoinduced state was stable up to 200 K (Figure S2), and the

[†] Institut de Chimie Moléculaire et de Matériaux d'Orsay, Université Paris Sud.

[‡] Université Bordeaux 1.

[§] Institut Néel.

[¶] Laboratoire de Physique des Solides, Université Paris Sud.

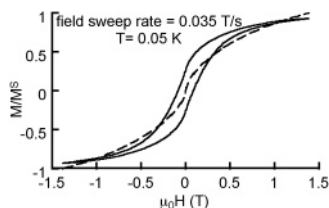


Figure 3. $M/M_S = f(\mu_0 H)$ on a PVP film of nanoparticles deposited on a microSQUID at 0.05 K before (---) and after (—) irradiation.

paramagnetic initial state was recovered after thermal treatment at 300 K.

Ac susceptibility measurements were performed after irradiation of the particles. As an out-of-phase component of the susceptibility was observed between 2 and 4 K (Figure S3), a micrometric portion of a PVP film containing the particles was studied in the 0.05–5 K range using a microSQUID. As expected, at $T = 0.05$ K, no hysteresis was observed before irradiation. The irradiation performed with a blue light diode (405 nm, power ~ 1 mW \cdot cm $^{-2}$) during 5 h leads to the opening of a hysteresis loop, with a coercive field of 920 Oe (Figure 3).

The coercive field (sweep rate of 0.035 T/s) reduces to zero above $T = 1$ K (Figure S4), which can either be a Curie temperature if the particles are multidomains or a blocking temperature if they are single domain. Relaxation measurements were performed in order to discriminate between both cases (Figure S5): at a given temperature, the magnetization was first saturated, the magnetic field was swept down to zero (at 0.14 T \cdot s $^{-1}$), and the magnetization decay was then measured as a function of time. The data were then scaled on a master curve (Figure S6), and the thermal dependence of the relaxation time τ extracted from the scaling process revealed two regimes (Figure S7). A temperature-activated regime is observed for $T > 0.3$ K that allows one to extract the effective energy barrier at zero field ($E_a/k = 6.7$ K) and the attempt time ($\tau_0 = 3 \times 10^{-6}$ s) corresponding to the Arrhenius law $\tau = \tau_0 \exp(-E_a/kT)$. The large τ_0 value corresponds to what is expected for superparamagnetic single-domain objects.⁵ Since the nanoparticles are diluted in a polymer matrix, dipolar interactions are weak and they can be considered as nearly non-interacting. Below 0.3 K, a temperature-independent regime was observed, suggesting the occurrence of quantum magnetic tunneling (QMT). This behavior is similar to that observed in many single-molecule magnets (SMMs).^{6a} Indeed, these 3 nm coordination particles can be described as giant clusters of about 55 ± 8 Ni^{II}Cu^IMo^V units ($S_{\max} = 82 \pm 12$). The size suppresses the steps usually seen on the hysteresis curve at zero field due to QMT. To obtain deeper understanding of the reversal of the magnetization, a method recently used for SMMs and single-chain magnets was applied to our sample (see Supporting Information).^{6b–d} It consists of measuring the temperature dependence of the coercive field H_c (field necessary to reverse the magnetization) at different sweep field rates $\nu = dH/dt$ (Figures S8 and S9). This set of experiments gave further evidence that the magnetization reversal is thermally activated for $T > 0.3$ K (Figure S10) and that E_a is close to 10 K (Figure S11), which is in good agreement with the value found (6.7 K) by the relaxation decay of the magnetization. All these experiments confirm that the irradiation process leads to a blocking of the magnetization, with a thermally activated behavior between 0.3 and 1 K and a tunneling of the magnetization below 0.3 K.

The optical spectrum measured after irradiation at 280 K ($T > 200$ K) shows the presence of the band associated with the Mo^{IV}–Cu^{II} charge transfer at 530 nm. At 10 K ($T < 200$ K), the intensity of this band decreases and another one appears at 710 nm associated with the Mo^V–Cu^I species, as already observed by Ohkoshi, Mathonière, and co-workers for the bulk compound (Figure S12).^{4c}

We have evidenced the first example of photoinduced superparamagnetic trimetallic CNP, with features indicating QMT at low temperature as observed in SMMs. Relaxation studies on one individual particle will be performed to confirm this phenomena. Other trimetallic CNPs are under investigation to raise the blocking temperature of such new bistable nanoobjects.

Acknowledgment. The authors thank the Centre National de la Recherche Scientifique, the French programme Nanoscience (ACI SupNanoMol NR0142), and the European community for financial support (Contract MRTN-CT-2003-504880/RTN Network “QuEMolNa”, contract NMP3-CT-2005-515767 NoE “MAGMA-NET”).

Supporting Information Available: UV–vis, $\chi_M T = f(T)$ in the 2–300 K range, ac data, and relaxation studies and related explanations (Figures S3–S12). This material is available free of charge via the Internet at <http://pubs.acs.org>.

References

- (1) (a) Vaucher, S.; Li, M.; Mann, S. *Angew. Chem., Int. Ed.* **2000**, *39*, 1793. (b) Vaucher, S.; Fielden, J.; Li, M.; Dujardin, E.; Mann, S. *Nano Lett.* **2002**, *2*, 225. (c) Dujardin, E.; Mann, S. *Adv. Mater.* **2004**, *16*, 1125.
- (2) Recent examples and references therein: (a) Galet, A.; Gaspar, A. B.; Muñoz, M. C.; Bukin, G. V.; Levchenko, G.; Real, J. A. *Adv. Mater.* **2005**, *17*, 2949. (b) Coronado, E.; Gimenez-Lopez, M. C.; Levchenko, G.; Romero, F. M.; Garcia-Baonza, V.; Milner, A.; Paz-Pasternak, M. *J. Am. Chem. Soc.* **2005**, *127*, 4580. (c) Kosaka, W.; Nomura, K.; Hashimoto, K.; Ohkoshi, S. I. *J. Am. Chem. Soc.* **2005**, *127*, 8590. (d) Ohkoshi, S. I.; Matsuda, T.; Tokoro, H.; Hashimoto, K. *Chem. Mater.* **2005**, *17*, 81.
- (3) (a) Catala, L.; Gacoin, T.; Boilot, J.-P.; Rivière, E.; Paulsen, C.; Lhotel, E.; Mallah, T. *Adv. Mater.* **2003**, *15*, 826. (b) Yamada-Sasano, M.; Arai, M.; Kurihara, M.; Sakamoto, M.; Miyake, M. *J. Am. Chem. Soc.* **2003**, *126*, 9482. (c) Kong, Q.; Chen, X. G.; Yao, J. L. *Nanotechnology* **2005**, *16*, 164. (d) Uemura, T.; Kitawaga, S. *J. Am. Chem. Soc.* **2003**, *125*, 7814. (e) Uemura, T.; Ohba, M.; Kitawaga, S. *Inorg. Chem.* **2004**, *43*, 7339. (f) Uemura, T.; Kitawaga, S. *Chem. Lett.* **2005**, *34*, 132. (g) Dominguez-Vera, J. M.; Colacio, E. *Inorg. Chem.* **2003**, *42*, 6983. (h) Gálvez, N.; Sánchez, P.; Domínguez-Vera, J. M. *Dalton Trans.* **2005**, *15*, 2492. (i) Clavel, G.; Guari, Y.; Larionova, J.; Guerin, C. *New J. Chem.* **2005**, *29*, 275. (j) Catala, L.; Gloter, A.; Stephan, O.; Rogez, G.; Mallah, T. *Chem. Commun.* **2006**, *9*, 1018. (k) Brinzei, D.; Catala, L.; Rogez, G.; Gloter, A.; Stephan, O.; Mallah, T. *J. Mater. Chem.* **2006**, *16*, 2593. (l) Guari, Y.; Larionova, J.; Guerin, C. *Chem.—Eur. J.* **2006**, *29*, 275. (m) Guari, Y.; Larionova, J.; Molvinger, K.; Folch, B.; Guerin, C. *Chem. Commun.* **2006**, 2613. (n) Kosaka, W.; Tozawa, M.; Hashimoto, K.; Ohkoshi, S. I. *Inorg. Chem. Commun.* **2006**, *9*, 920.
- (4) (a) Moore, J. G.; Lochner, E. J.; Ramsey, C.; Dalal, N. S.; Stiegman, A. E. *Angew. Chem., Int. Ed.* **2003**, *42*, 2741. (b) Catala, L.; Mathonière, C.; Gloter, A.; Stephan, O.; Gacoin, T.; Boilot, J.-P.; Mallah, T. *Chem. Commun.* **2005**, *6*, 746. (c) Ohkoshi, S. I.; Tokoro, H.; Hozumi, T.; Zhang, Y.; Hashimoto, K.; Mathoniere, C.; Bord, I.; Rombaut, G.; Verelst, M.; Cartier dit Moulin, C.; Villain, F. *J. Am. Chem. Soc.* **2006**, *128*, 270 and references therein.
- (5) Dormann, J. L.; Fiorani, D. *J. Magn. Magn. Mater.* **1995**, *140*, 415.
- (6) (a) Gatteschi, D.; Sessoli, R. *Angew. Chem., Int. Ed.* **2003**, *42*, 268. (b) Wernsdorfer, W.; Murugesu, M.; Tasiopoulos, A. J.; Christou, G. *Phys. Rev. B* **2005**, *72*, 212406. (c) Wernsdorfer, W.; Clérac, R.; Coulon, C.; Lecren, L.; Miyasaka, H. *Phys. Rev. Lett.* **2005**, *95*, 237203. (d) Costes, J.-P.; Auchel, M.; Dahan, F.; Peyrou, V.; Shova, S.; Wernsdorfer, W. *Inorg. Chem.* **2006**, *45*, 1924.

JA068451S